

# Structural fingerprints of electronic change in the phase-change-material: $\text{Ge}_2\text{Sb}_2\text{Te}_5$

B. Cai,<sup>1</sup> D. A. Drabold,<sup>1,a)</sup> and S. R. Elliott<sup>2</sup>

<sup>1</sup>Department of Physics and Astronomy, Ohio University, Athens, Ohio 45701, USA

<sup>2</sup>Department of Chemistry, University of Cambridge, Cambridge, CB2 1EW, United Kingdom

(Received 21 September 2010; accepted 23 October 2010; published online 10 November 2010)

In this paper, we generate a- $\text{Ge}_2\text{Sb}_2\text{Te}_5$  models via *ab initio* molecular dynamic simulations, track the dynamic changes of network at 500 K, and correlate the structural changes in the course of the simulation with changes in electronic structure. Considerable fluctuations of the electronic gap are observed even for a model in equilibrium. We compare our study to experiments and other simulations. © 2010 American Institute of Physics. [doi:10.1063/1.3516039]

For Ge–Sb–Te alloys, there exists a rapid and reversible transition between crystalline and amorphous states. Controlled modification of electrical conductivity and optical properties of the transition is the basis for promising flash and optical memory devices. Akola and Jones<sup>1</sup> analyzed the structure of liquid and amorphous phases and compared the electronic structure with the crystal phase. In 2008, Hegedus and Elliott<sup>2</sup> reproduced the crystal-amorphous transition by molecular dynamics simulation, and they found that the rapid nature of the transition was due to the presence of crystal fragments—four member square rings (so-called “seeds”) in amorphous and liquid phases. Their work provided a way to track the dynamic changes of network topology and electronic structure at the same time. Welnic and co-workers<sup>3</sup> studied the origin of optical properties and argued that the optical contrast between amorphous and crystalline phases is due to a change in local order of Ge atoms. Despite this progress, the correlation between topology and electronic structure, most especially the origin of the change in the electronic gap, is still imperfectly understood. One of the challenges is the basic limitation of the LDA for estimating the gap.

We began our work by creating amorphous  $\text{Ge}_2\text{Sb}_2\text{Te}_5$  models by using the VIENNA *AB INITIO* SIMULATION PACKAGE (VASP)—a plane-wave density functional theory (DFT) code, using a projector augmented wave potential and the generalized gradient approximation–Perdew–Burke–Ernzerhof method.<sup>4</sup> 63-atom amorphous  $\text{Ge}_2\text{Sb}_2\text{Te}_5$  models were made as follows. The system was first melted and equilibrated at 1000 K, followed by a rapid quench to 500 K with a quench rate of 16 K/ps. Then the system was equilibrated for 20 ps, and data collection began at 10 ps.

The calculated atomic coordinations for a- $\text{Ge}_2\text{Sb}_2\text{Te}_5$  (500 K) and l- $\text{Ge}_2\text{Sb}_2\text{Te}_5$  (1000 K) are listed in Table I with a 3.2 Å cutoff. These results are similar to those in Ref. 1, although in our case, the mean coordination of Ge atoms is slightly increased after thermal quench and equilibration, which may be due to the higher equilibration temperature used and/or size artifacts for our smaller model. More highly coordinated Ge and Sb (fivefold and sixfold) atoms appeared in the amorphous phase, which suggests that a near-octahedral structure may be formed (square-rings and eight-atom cubes). These results indicate that structural ordering is

enhanced in the amorphous phase relative to the liquid. Moreover, considering the chemical order, the number of wrong bonds (Te–Te, Ge–Ge, Sb–Sb, and Ge–Sb) is decreased from 1000 to 500 K, which indicates that the chemical order is also improved. The average number of seeds (four member square rings) shows an increase in the amorphous phase, and more than 50% of the atoms are involved in seeds, compared to only 10% in the liquid phase. The calculated partial radial distribution functions are plotted in Fig. 1. The first peak in the Te–Ge and Te–Sb partials are located at 2.81 and 2.92 Å. The shallow first minima imply that the coordination is sensitive to the cutoff value selected. The Te–Ge partial has a broad and weak second peak. However, the Te–Sb partial possesses a second peak with a maximum at 4.4 Å, which indicates that Ge and Sb atoms differ in local environment relative to Te atoms. Regarding the homopolar bonds, there is a major peak for the Sb–Sb partial centered at 2.9 Å. These results are similar to other simulations<sup>1</sup> and also experimental results.<sup>4</sup>

The electronic structure is analyzed through the electronic density of states (EDOS) obtained from Hartree–Fock (HF) calculations. HF is used only to analyze the EDOS, not for forces and total energies. HF is known to exaggerate both the optical gap and charge fluctuations in the electron gas. These features are helpful to us here for diagnosing structural correlations. In the following discussion, the calculated EDOS is averaged over 1000 configurations from the last 2 ps when the cell is in thermal equilibrium at a fixed temperature of 500 K. Finally, the averaged HF result of the amorphous phase gives an electronic gap around 0.4 eV, which is wider than the DFT result (0.2 eV) (Ref. 1) and is closer to the experimental value (0.7 eV).<sup>5</sup> Although the gap is still smaller than the experimental value, it is much improved over LDA, and this may imply that HF provides a better

TABLE I. Mean coordinations, bond types, and seeds (four member square rings) statistics at 500 K. The result obtained at 1000 K is listed in brackets (coordination cutoff=3.2 Å).

	$N_{\text{tot}}$	$N_{\text{Te}}$	$N_{\text{Ge}}$	$N_{\text{Sb}}$
Te	3.4 (3.0)	20% (30%)	47% (41%)	33% (29%)
Ge	4.6 (4.3)	86% (71%)	5% (13%)	9% (16%)
Sb	4.1 (3.6)	69% (62%)	11% (20%)	20% (18%)
$N_{\text{seed}}$	18 (1.8)	52% (10%)	69% (12%)	53% (10%)

<sup>a)</sup>Electronic mail: drabold@ohio.edu.

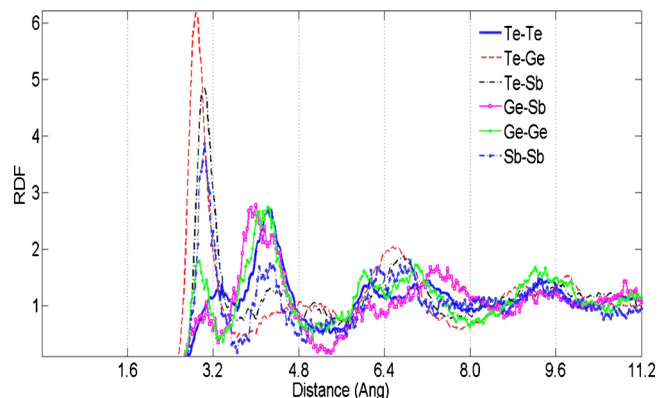


FIG. 1. (Color online) Partial radial distribution functions for a-Ge<sub>2</sub>Sb<sub>2</sub>Te<sub>5</sub>.

starting point for analysis of the electronic structure.

To correlate topology with electronic structure, we projected the EDOS onto different local sites and are able to attribute the electronic states to specific structural units. We first show the averaged EDOS for different species and orbitals in Fig. 2. The key findings are that, for all three species, p orbitals dominate the gap and tail states; if considering the species, Te-p, Sb-p, Ge-p, Ge-s, and Sb-s are important in determining tail states and the magnitude of the gap (Fig. 2). To further correlate structural oddities with electronic states, we also sort atoms with specific features into different groups and accumulate the contribution to EDOS. We briefly report that groups forming homopolar or heteropolar bonds showed that there is a significant difference at a “deep gap” around  $-7$  eV below the Fermi level (0 eV) in EDOS (atoms involved in heteropolar bonds form a bigger deep gap); however, atoms forming homopolar bonds have a minor impact on tail states and the electronic gap near the Fermi level. Considering the coordination, for Te, twofold Te atoms contribute to a narrowed gap and conduction-band tail states appear; for Ge atoms, the contributions for three-, four-, five-, and sixfold atoms are almost the same; for Sb atoms, the conduction-band tail of sixfold Sb atoms is pushed to a low-energy level, and the valence-band tail associated with threefold Sb atoms, which satisfy the “8-N” rule, is pushed into a higher energy region. While there are differences in electronic tail states and the gap value associated with coordination numbers, the influence is fairly weak. Similarly, sorting atoms involved in seeds or not also showed a minor impact on gap magnitude and tail states.

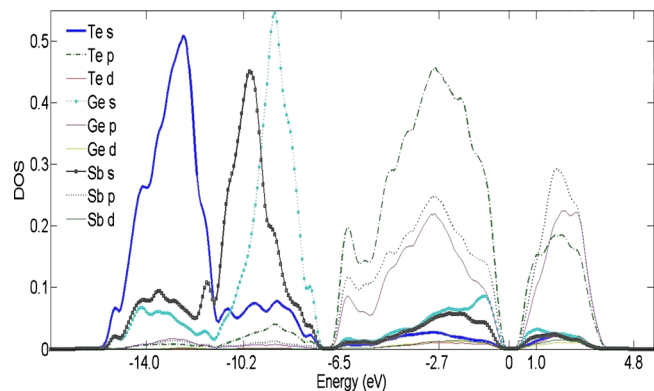


FIG. 2. (Color online) Electronic densities of states projected onto different atomic species and orbitals. The Fermi level is at 0 eV.

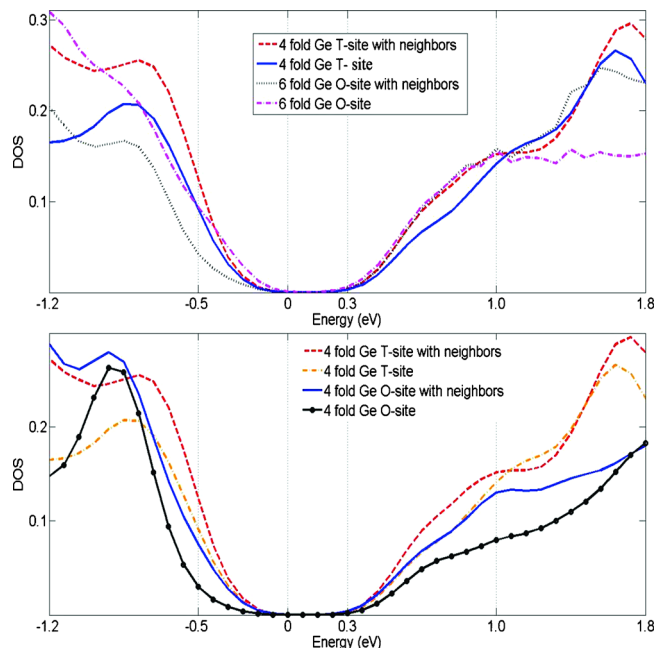


FIG. 3. (Color online) Projected EDOS on Ge atoms at tetrahedral and octahedral sites. “T” and “O” represent tetrahedral and octahedral sites. The “Ge-T/O site” plot only considers the contribution of Ge atoms to the EDOS, while the “Ge-T/O site with neighbors” plot contains the contribution of Ge atoms and their neighbors. The Fermi level is at 0 eV.

We also considered the “umbrella flip” of Ge atoms. We compared the EDOS of Ge atoms sitting at octahedral sites (O-site) and tetrahedral sites (T-site), as we illustrate in Fig. 3. The projected EDOS on Ge atoms and their neighbors are all considered. The results indicate that sixfold octahedral Ge and tetrahedral Ge have a similar local gap. However, fourfold Ge at an octahedral site (four neighbors with  $90^\circ$  angles) has both a shifted valence-band tail and conduction-band tail, which may result in a bigger gap. Thus, from our result,  $sp^3$  hybrids introduced by a Ge umbrella-flip may not be the reason for an increased gap in the amorphous phase, but the octahedral Ge existing in the amorphous phase at least would not increase the electronic gap. Analysis of Ge<sub>1</sub>Sb<sub>2</sub>Te<sub>5</sub> showed a similar result.<sup>6</sup>

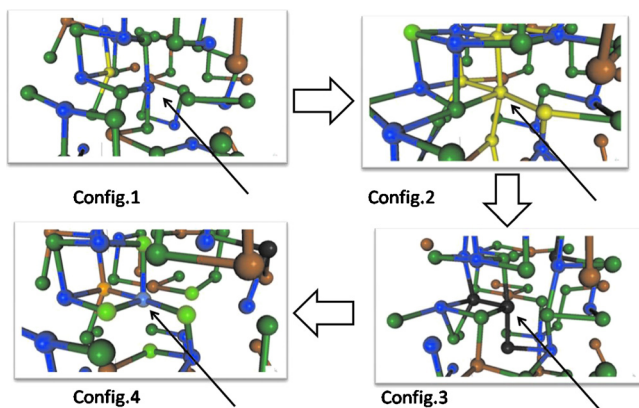


FIG. 4. (Color online) Snapshots of topology changes for one Ge atom and its six neighbors (Ge, blue/darkest; Sb, brown/next darkest; and Te, green/light). The central Ge atom is identified by black arrows. In monochrome: for Config. 2, the valence tail states are localized on the lightest (yellow) atoms connected to the central atom and in Config. 3 conduction tail states are localized on dark (black) atoms connected to the central atom.

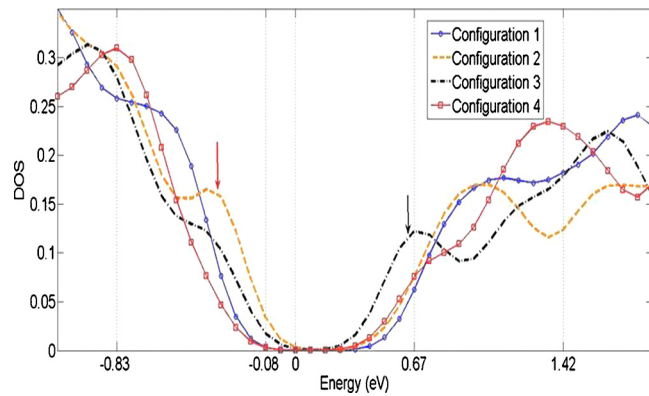


FIG. 5. (Color online) Instantaneous snapshots of EDOS correlated with the configurations of Fig. 4. A smaller gap appear in Configs. 2 and 3. The valence-band tail states (orange arrow) are associated with yellow atoms in Config. 2 of Fig. 4. The conduction-band tail states (black arrow) are associated with black atoms in Config. 3 of Fig. 4. The Fermi level is at 0 eV.

Next, we performed a dynamic analysis for a- $\text{Ge}_2\text{Sb}_2\text{Te}_5$ . We tracked the structure and the electronic gap during a quench from 1000 to 500 K with thermal equilibration at 500 K. Significant structural changes started to occur after 24 ps (the temperature was then near 640 K). The number of homopolar bonds dropped, the number of four-membered rings increased, and the mean coordination increased. The changes in topology are similar to those reported in Ref. 2, and all these shifts signal an increase of both chemical order and structural order. The electronic gap, which we take to be the difference between lowest unoccupied and highest occupied molecular orbital levels, increased overall, but we observed that there are considerable fluctuations even for the well-equilibrated system. Local geometry may have huge effects on the gap.<sup>7</sup>

To study how changes in the local environment at a specific site affected the electronic gap, we tracked a specific unit in the system during equilibration, and we show such an evolution for both the topology and the electronic structure in Figs. 4 and 5. We mainly focused on one Ge atom, which occupied a near-octahedral site (six nearest Te neighbors with around  $90^\circ$  bond angles, indicated by a black arrow in Fig. 4) and its six nearest neighbors. We correlated their

coordinations and electronic density of states together for many time steps. Configurations 1 and 4 exhibit the biggest gap. However, at intermediate steps between configurations 1 and 4, tail states appear. At configuration 2, a valence-band tail state was present, and it was mainly localized on the central Ge atom and four of its nearest neighbors (yellow atoms in Config. 2 of Fig. 4); at configuration 3, a conduction-band tail appears, mainly localized on the center Ge atom and two of its nearest neighbors (black atoms in Config. 3 of Fig. 4). We should emphasize that from configurations 1–4, the whole network did not experience a major change, but the electronic gap fluctuates. Thus, the appearance of valence-band and conduction-band tails is strongly associated with distortions at this Ge site. Our simulations emphasize the dynamic nature of the electronic band tails in  $\text{Ge}_2\text{Sb}_2\text{Te}_5$ .

In conclusion, we made  $\text{Ge}_2\text{Sb}_2\text{Te}_5$  models with a “quench from melt” method. HF calculations give a 0.4 eV electronic gap of the amorphous phase. We found that Te-p, Sb-p, Ge-p, Ge-s, and Sb-s orbitals are most important to tail states and affect the magnitude of the gap. Sixfold octahedral Ge and fourfold tetrahedral Ge give rise to similar gaps, but fourfold octahedral Ge results in a bigger gap with both shifted valence-band and conduction-band tails. The study also reveals a large fluctuation in gap value during thermal equilibration.

B.C. would like to thank Dr. J. Hegedus for an introduction to this area. This work was partly supported by the U.S. NSF under Grant Nos. DMR-09033225 and DMR-0844014.

<sup>1</sup>J. Akola and R. O. Jones, *Phys. Rev. B* **76**, 235201 (2007); *J. Phys.: Condens. Matter* **20**, 46103 (2008).

<sup>2</sup>J. Hegedüs and S. R. Elliott, *Nature Mater.* **7**, 399 (2008).

<sup>3</sup>W. Welnic, S. Botti, L. Reining, and M. Wuttig, *Phys. Rev. Lett.* **98**, 236403 (2007).

<sup>4</sup>M. Naito, M. Ishimaru, Y. Hirotsu, R. Kojima, and N. Yamada, *J. Appl. Phys.* **107**, 103507 (2010).

<sup>5</sup>B. S. Lee, J. R. Abelson, S. G. Bishop, D. H. Kang, B. Cheong, and K. B. Kim, *J. Appl. Phys.* **97**, 093509 (2005).

<sup>6</sup>J. Y. Raty, C. Otjacques, J. P. Gaspard, and C. Bichara, *Solid State Sci.* **12**, 193 (2010).

<sup>7</sup>M. Wuttig, D. Lusebrink, D. Wamwangi, W. Welnic, M. Gilleben, and R. Dronskowski, *Nature Mater.* **6**, 122 (2007).